

Analysis of Stress Distribution Around Defects and Inclusions by F.E.M.

Sam-Hong Song* and Jin-Bong Kim**

(Received March 26, 1995)

This study has been made to investigate the stress distribution around defects and inclusions that behave as stress concentrators. The stress distribution and interaction effects around defects and inclusions were analyzed using Finite Element Method.

Key Words: Finite Element Analysis, Inclusion, Stress Interaction, Stress Concentration

1. Introduction

The effect of defects and inclusions on the behavior of fatigue crack depends on the hardness of base material. However, if fatigue cracks initiate from these defects and inclusions then local areas including these become stress concentrator(Brooksank et al., 1972 ; Trantina et al., 1984 ; Sam Hong Song et al., 1985 ; Sam Hong Song et al., 1987a), and accordingly it is expected that the fatigue strength is affected by size and configuration of defects and inclusions. As it needs lots of time and effort to produce specimen controlled the size and configuration of defects and inclusions metallurgically , so the characteristic of micro defects is studied using artificial defects instead of natural defects.

Size and configuration of defects and inclusions in material is various and the interval between them is near and far(Sam Hong Song, 1987b). Specially, if the interval between them is near then there are singular stress field by stress interaction(Horii et al., 1985 ; Yatsuda et al., 1985) and fatigue cracks propagate rapidly(Murakami et al., 1983 ; Heath et al., 1984 ; Miyoshi et al., 1985 ; Roger, 1982). Accordingly, the analysis of stress distribution between defects is required to estimate the interaction effect between defects or cracks. However, as

there are few exact solutions for stress distribution around defects and cracks, stress concentration diagram for the two dimensional configuration by Peterson(Peterson, 1962) based on the results by Neuber(1957) is used. It is pointed out that there are lots of errors using these results to three dimensional problems. Lots of results for the stress distribution of 3-dimensional problem are reported to minimize the error and approximate the real problems.

These results can be classified into experimental method and analytical method, and problems are as follows . Measurement of stress at the surface of material is possible, but it is impossible at the inner part of material by experimental method(Brooksank et al., 1972), and configurations of defect and inclusion are spherical, semi-spherical, or semi-ellipsoid in analytical method(Fujita et al., 1980). However those results can't be applied to the case with cylindrical shape which is used in the study of artificial micro hole problems. The analytic result of stress distribution for the cylindrical defect is reported only by H. Noguchi(Nisitani, H. et al., 1988). According to artificial micro hole problems with cylindrical configuration , the stress behaviour and stress interaction effect on initiation and propagation of cracks have been studied(Sam Hong Song et al., 1990 ; S. H. Song et al., 1992) by authors sequentially.

Considering problems mentioned above, stress distribution for the cylindrical inclusions or defects are analyzed by F.E.M. and stress interac-

* Korea University

** Korea Electrotechnology Research Institute

inclusions and defects as follows.

- (1) The shape of inclusions and defects is cylindrical.
- (2) Inclusions are completely bonded with base material.
- (3) Young's modulus of base material (E_M) is 196 GPa and that of inclusions(E_I) are higher or lower than E_M . E_I of Alumina(392 GPa) is used for the higher one and E_I of Sulphide or Calcium Aluminate(96 GPa) is used for the lower one.

For the special case of $E_I/E_M=0$, it means the cavity that there is separation or crush between the base material and inclusion. The stress interaction between inclusions whose Young's modulus are different is analyzed.

- (4) In order to investigate the interaction of stress between inclusions, the distance between the centers of the inclusions is varied.

3. Results and Discussion

3.1 Stress distribution around inclusions

The stress component σ_y around two same inclusions divided by nominal stress σ_0 are as shown in Fig. 4~Fig. 7. In the cases, the depth of inclusions are twice the radius r and the interval

between the edge of inclusions is $2r$.

Figure 4 and Figure 5 represent the cases that Young's modulus ratio at $A-B$ equals 0 and that of $C-D$ is 0.5 and 2. Considering the results, σ_y/σ_0 in inclusions is lower than 1 and σ_y/σ_0 in base material at the points C, D are higher than 1 for $E_I/E_M < 1$, and the maximum value of σ_y/σ_0 in base material increases to 2.9 for $E_I/E_M=0$. However σ_y/σ_0 in inclusions is higher than 1 and σ_y/σ_0 in base material at points C, D are lower than 1 for $E_I/E_M > 1$, and σ_y/σ_0 in base material is higher than 1 at the point E .

Figs. 6 and 7 represent the cases that the two equal inclusions are located. The maximum stress points are B, C , or A, B, C, D according to

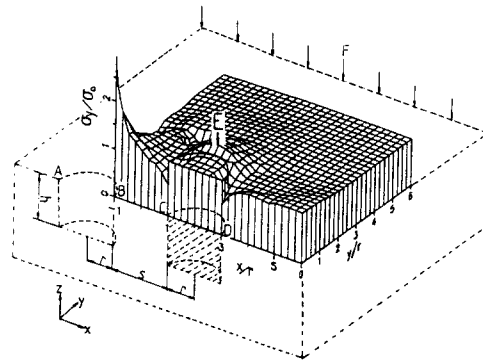


Fig. 5 σ_y distribution around inclusions on the upper surface($E_I/E_M=0$; A-B, $E_I/E_M=2$; C-D, E_I ; elasticity modulus of inclusion, E_M ; elasticity modulus of base material, σ_0 ; nominal stress)

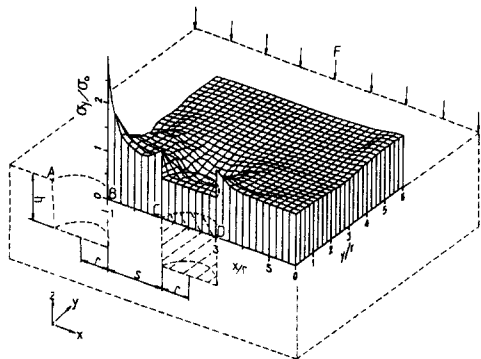


Fig. 4 σ_y distribution around inclusions on the upper surface($E_I/E_M=0$; A-B, $E_I/E_M=0.5$; C-D, E_I ; elasticity modulus of inclusion, E_M ; elasticity modulus of base material, σ_0 ; nominal stress)

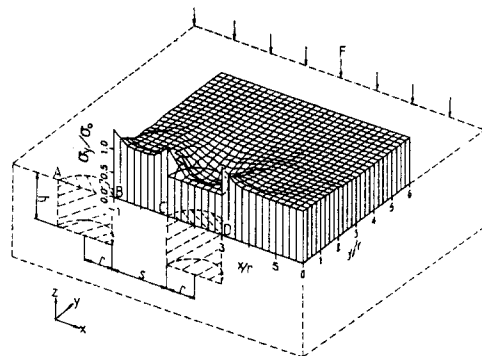


Fig. 6 σ_y distribution around inclusions on the upper surface($E_I/E_M=0.5$; A-B, C-D, E_I ; elasticity modulus of inclusion, E_M ; elasticity modulus of base material, σ_0 ; nominal stress)

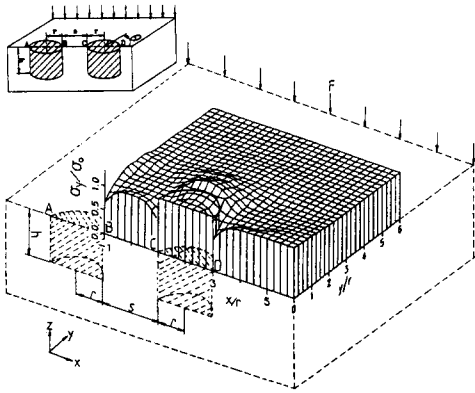


Fig. 7 σ_y distribution around inclusions on the upper surface($E_I/E_M=2$; A-B, C-D, E_I ; elasticity modulus of inclusion, E_M ; elasticity modulus of basematerial, σ_0 ; nominal stress)

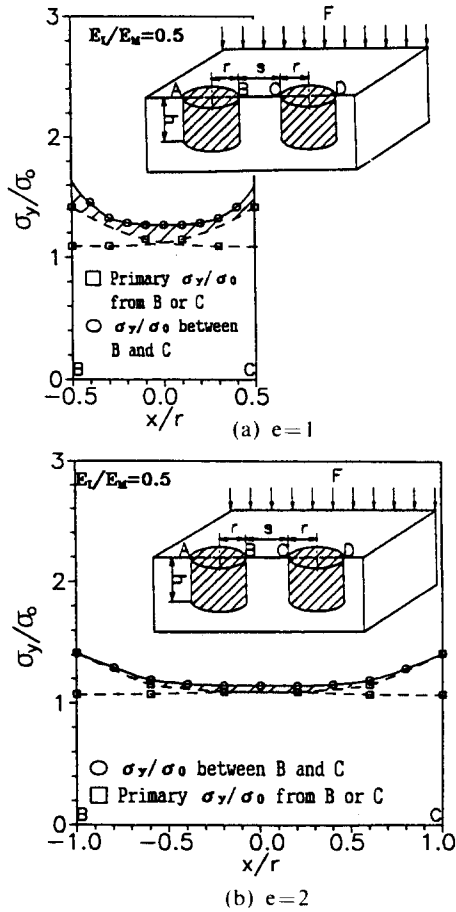


Fig. 8 σ_y distribution of IT_{05} between inclusions on the upper surface($E_I/E_M=0.5$; A-B, C-D, $e = s/r=2$)

the space between inclusions for $E_I/E_M=0.5$ as shown in Fig. 6. In these cases, as the stress distribution is symmetric with respect to $x/r=0$, the stress distribution of left side from the point B is not displayed. On the other hand, the maximum stress points are not A, B, C, D as shown in Fig. 6, but the points which is rotated $\pm 90^\circ$ from points D and B about the axis of each inclusions($x/r = \pm 2$).

3.2 Stress interaction between twin inclusions

The stress interaction effects between twin inclusions are as shown in Fig. 8~Fig. 12. \circ represent values for the stress distribution arisen

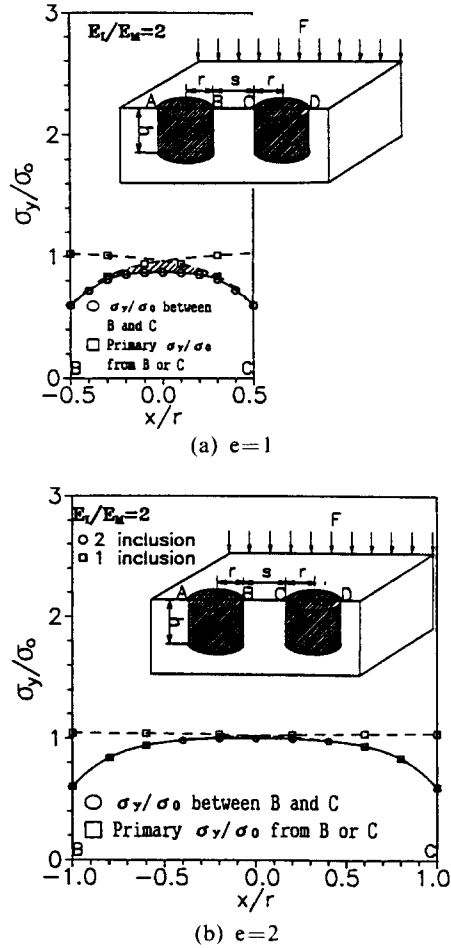


Fig. 9 σ_y distribution of IT_2 between inclusions on the upper surface($E_I/E_M=2$; A-B, C-D, $e = s/r=2$)

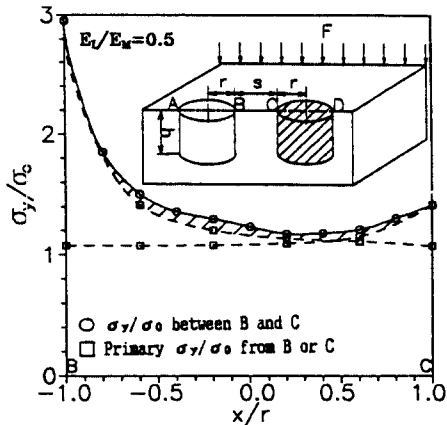


Fig. 10 σ_y distribution of IT_{005} between inclusions on the upper surface($E_I/E_M=0$; A-B, $E_I/E_M=0.5$; C-D, $e=s/r=2$)

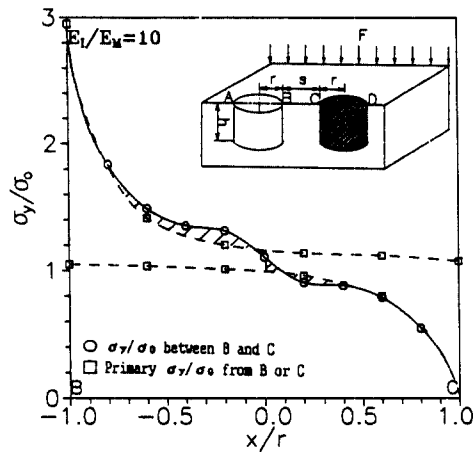


Fig. 12 σ_y distribution of IT_{02} between inclusions on the upper surface($e=2$, $E_I/E_M=0$; A-B, $E_I/E_M=10$; C-D)

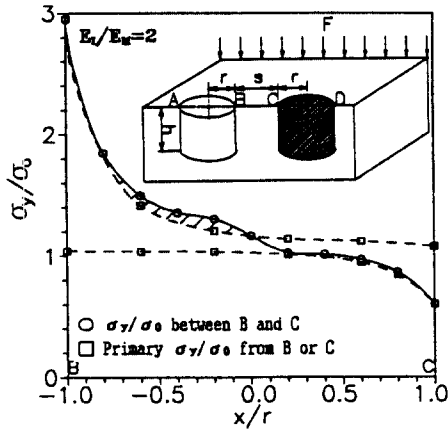


Fig. 11 σ_y distribution of IT_{02} between inclusions on the upper surface($E_I/E_M=0$; A-B, $E_I/E_M=2$; C-D, $e=s/r=2$)

0.8 in model IT_{05} as shown in Fig. 8. For the case of the model IT_{02} , the stress affects each other in the region of $-0.4 \leq x/r \leq 0.4$ for $e=1$, and $-0.2 \leq x/r \leq 0.2$ for $e=2$. Comparing the results with Fig. 7, the stress interacting effect decreases as the ratio of E_I/E_M increases.

As the distance between two inclusions with $E_I/E_M=0$ and $E_I/E_M \neq 0$ becomes near, the stress interaction effect is more intensive in the region near the inclusion with $E_I/E_M \neq 0$ than the region near the inclusion with $E_I/E_M=0$ for the model IT_{005} and IT_{02} as shown in Figs. 10~12. The stress interaction effect for the region of $E_I/E_M=0$ ($-1 \leq x/r \leq 0$) is almost constant with the variation of E_I/E_M from 0.5 to 10, and that of $E_I/E_M \neq 0$ decreases gradually as E_I/E_M becomes high.

by two inclusions, and \square represents that of a inclusion arisen by each independent inclusion. The deviant crease lines represent the area where the stress affects each other.

When the two inclusions are spaced in such a manner that their two closest points are separated by a distance of inclusion radius($e=1$), stress distribution is affected by a opposite inclusion in all the closest region, and if two closest points are separated by twice the distance of a inclusion radius($e=2$), stress distribution is affected by a opposite inclusion in the region of $-0.8 \leq x/r \leq$

3.3 Stress interaction between unequal size inclusions

The stress interaction effects between two unequal size inclusions are as shown in Fig. 13 and Fig. 14. \circ represents the stress distribution between twin inclusions and \blacksquare represents the stress distribution between unequal size inclusions. \triangle represents the independent stress distribution arisen by one inclusion at A and B. In these cases, solid lines represents the stress distribution line arisen by two inclusions and dashed

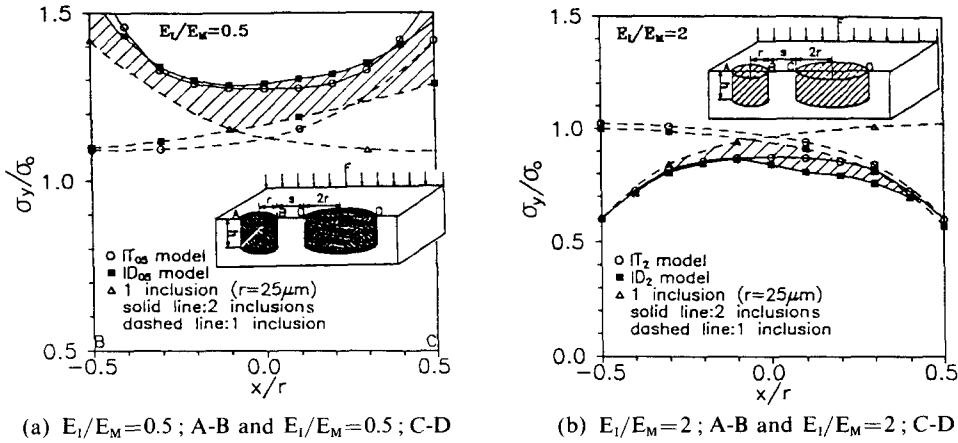


Fig. 13 σ_y distribution between unequal size inclusions on the upper surface($e=1$)

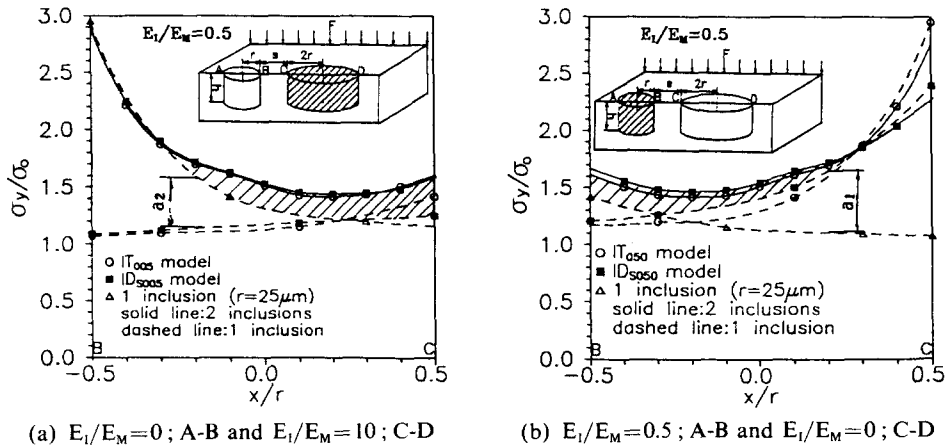


Fig. 14 σ_y distribution between unequal E_1 and size inclusions on the upper surface($e=1$)

lines represent the independent stress distribution line arisen by each inclusions. In addition, deviant crease lines represent the area where the stress affects each other.

The stress interaction effects between twin inclusions whose Young's modulus are equal is as shown in Fig. 13. Comparing the results, σ_y/σ_0 of ID_{05} is higher than that of the model IT_{05} at $-0.35 \leq x/r \leq 0.35$ for $E_1/E_M=0.5$ and σ_y/σ_0 of ID_2 at $-0.5 \leq x/r \leq 0.5$ for $E_1/E_M=2$. The reason why the difference in σ_y/σ_0 between IT series and ID series for $E_1/E_M=2$ is opposite to $E_1/E_M=0.5$ is that the stress increasing factors for $E_1/E_M < 1$ becomes the stress decreasing factors with stress variation by the stress interaction. In addi-

tion, the reason why σ_y/σ_0 of ID_{05} is higher than that of IT_{05} at $-0.35 \leq x/r \leq 0.35$ for $E_1/E_M=0.5$ and σ_y/σ_0 of ID_2 is lower than IT_2 is that the stress interaction effect of ID series is higher than that of IT series due to the fact that the stress concentration of IT series is more localized than that of ID series. From the results, it can be extracted that the stress interaction effect at large inclusion side is higher than at small inclusion side.

σ_y/σ_0 distribution between two inclusions which Young's modulus ratio is 0 and 0.5 are represented as shown in Fig. 14. σ_y/σ_0 of ID series is higher than that of IT series and the stress interaction effect of inclusion side is higher

than that of inclusion side and that of model ID_{s005} is higher than that of model ID_{s050} .

The difference of stress interaction effect between model ID_{s050} and ID_{s005} is due to the difference of stress arisen by each independent inclusions. As $a_1 > a_2$ (a_1 at $x/r=0.2$, a_2 at $x/r=-0.2$) which is the stress difference between independent inclusions of ID_{s050} or ID_{s005} , so the stress interaction effect become high if the stress difference between independent inclusions become small.

From the above results, we can notice that the stress interaction effect depends on the stress distribution pattern and the stress difference between inclusions if the inclusions which are

different in dimension and Young's modulus are spaced adjacently and the stresses arisen by each inclusion affect each other.

3.4 Comparison between experiment and analysis results

In order to elucidate the effect of stress distribution on the fatigue crack propagation emanating from defects, rotary bending tests were carried out on the specimens with micro defects as follows ;

- (a) single micro hole : $d=300 \mu\text{m}$, $h=300 \mu\text{m}$ (IS model)
- (b) twin micro holes : $d=300 \mu\text{m}$, $h=300 \mu\text{m}$, $s=300 \mu\text{m}$ (IT model)
- (c) unequal micro holes : $d=300 \mu\text{m}$, $d_2=500$

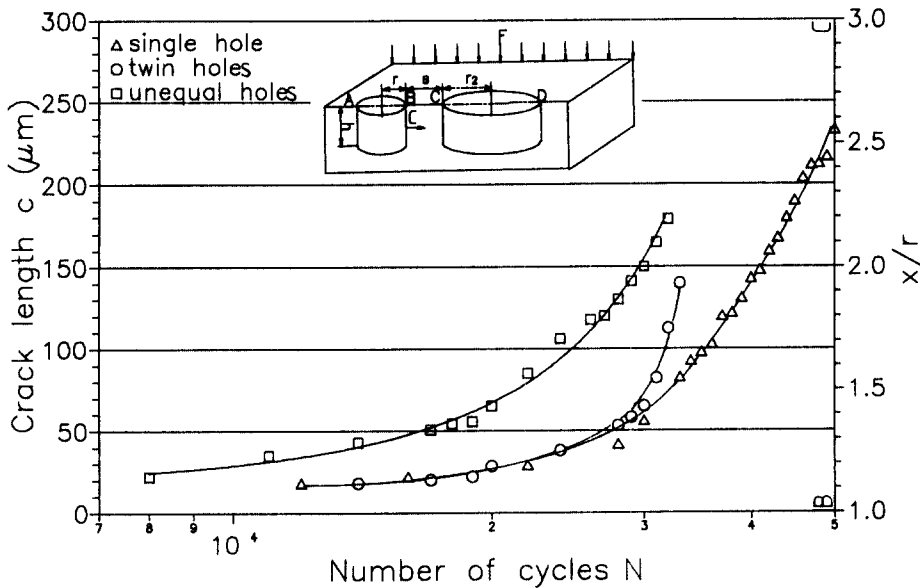


Fig. 15 Crack growth curve(c =crack length from B)

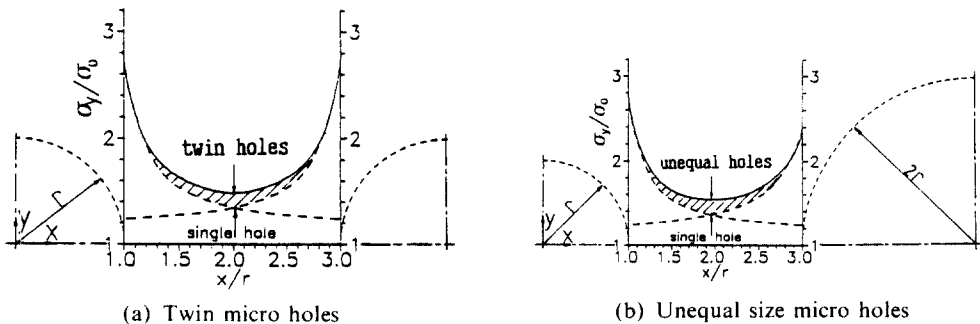


Fig. 16 σ_y/σ_0 distribution between micro holes($h/r=2$, $e=s/r=2$)

μm , $h=300\ \mu\text{m}$, $s=300\ \mu\text{m}$ (*ID* model)

Figure 15 represents the relation between the crack length from the point B and number of stress cycles. The crack length of the model *IT* is shorter than that of the model *ID* at the same number of stress cycles, and the crack length of the *IT* model and the model *IS* is equal until $N=2.3 \times 10^4$ cycles; that is, in the range of $x/r \leq 1.2$. However the crack length of the *IT* model is larger than that of the model *IS* at $x/r > 1.2$.

Figure 16 represents σ_y/σ_0 analyzed by F.E.M. in the model *IT* and the model *ID*. σ_y/σ_0 in the model *ID* is larger than that in the model *IT* around $x/r=1$ and the stress interaction in the model *IT* affects in the range of $1.2 \leq x/r \leq 2.8$.

Comparing the results between two methods, we can notice that the stress distribution between micro holes affects the behavior of fatigue crack propagation.

4. Conclusions

The stress distribution and interaction effect between inclusions are obtained to investigate the behavior of defects or inclusions as stress concentrators. The Young's modulus ratio (E_I/E_M) between base material and inclusions has been considered.

On the basis of the results which have been presented, several conclusions are extracted as follows:

(1) The maximum stress in base material side which is in contact with inclusion for $E_I/E_M < 1$ is occurred at $\theta = \pm 90^\circ$. However the point moves to $\theta = 0^\circ$ and 180° for $E_I/E_M > 1$.

(2) When a defect and an inclusion are spaced in such a manner that the stress distribution is affected by an opposite one, the interaction effect of σ_y is higher in inclusion side than in defect side.

(3) σ_y between different size inclusions except the limited region around a large inclusion is higher than that of twin inclusions for $E_I/E_M < 1$, but it is reversed for $E_I/E_M > 1$.

(4) When the distance between inclusions or defects which are different in size and Young's modulus is near, if the difference of σ_y arised by

inclusions is small, the stress interaction effect is high. However, if the difference of σ_y is large, the stress interaction effect is low.

References

Brooksank, D. and Andrews, K. W., 1972, "Stress Fields around Inclusions and their Relation to Mechanical Properties," *Journal Iron & Steel Inst.* pp. 246~255.

Fujita, T., Tsuchida, E. and Nakahara, I., 1980, "Stress Concentration due to a Hemi-Prolate Spheroidal Pit at a Free Surface of a Semi-Infinite Body under All-around Tension," *Bulletin of the JSME*, Vol. 23, No. 181, pp. 1048~1054.

Heath, B. J. and Grand, Jr., A. F., 1984, "Stress Intensity Factors for Coalescing and Single Corner Flaws Along a Hole Bore in a Plate," *Engineering Fracture Mechanics*, Vol. 19, No. 4, pp. 665~673.

Horii, H. and Nemat-Nasser, S., 1985, "Elastic Fields of Interacting Inhomogeneities," *Int. J. Solids Structures*, Vol. 21, No. 7, pp. 731~745.

Miyoshi, T., Shiratori, M. and Tanabe, O., 1985, "Stress Intensity Factors for Surface Cracks with Arbitrary Shapes in Plates and Shells," *Fracture Mechanics*, 16th Symposium, ASTM STP868, pp. 521~534.

Murakami, Y. and Nemat-Nasser, S. 1983, "Growth and Stability of Interacting Surface-Flaws of Arbitrary Shape," *Engineering Fracture Mechanics*, Vol. 17, No. 3, pp. 193~210.

Neuber, H., 1957, *Theory of Notch Stresses*, Springer, Berlin.

Nisitani, H., etc., 1988, "Tension in Semi-Infinite Body with Drill Hole Shape Pit," *Trans. J. S.M.E.*, Vol. 54, No. 501, pp. 977~982.

Peterson, R. E., 1962, *Stress Concentration Design Factors*, John-Wiley & Sons.

Roger Chang, 1982, "On Crack-Crack Interaction and Coalescence in Fatigue," *Engineering Fracture Mechanics*, Vol. 16, No. 5, pp. 683~693.

Sam Hong Song and Jin Bong Kim, 1990, "3-D Analysis of Stress Distribution Around Inclusion by F.E.M.," *Trans. of the KSME*, Vol. 15, No. 5, pp. 1462~1471.

Sam Hong Song and Whan Sub Oh, 1985, "Fatigue Crack Behavior Emanating from Surface Defects," *Trans. of the KSME.*, Vol. 9, No. 2, pp. 150~157.

Sam Hong Song and Whan Sup Oh, 1987a, "Behavior of Initiation and Propagation of Fatigue Cracks Around Microholes," *Trans. K.S. M.M.E.*, Vol. 1, No. 2, pp. 250~258.

Sam Hong Song and Whan Sup Oh, 1987b, "Behavior of Initiation and Propagation of Fatigue Cracks Around Microhole," *Proc. of the First Conference on Mechanical Behaviours*, pp. 251~258.

Song, S. H. and Kim, J. B., 1992, "Analysis of

the Stress Distribution around Flaws and the Interaction Effects between Fatigue Cracks by F. E.M.," VII *International Congress on Experimental Mechanics and Manufacturers Exhibit*, pp. 200~204.

Trantina, G. G. and Barishpolsky, M., 1984, "Elastic-Plastic Analysis of Small Defect-Void and Inclusion," *Engng. Fracture Mech.*, Vol. 20, No. 1, pp. 1~10.

Yatsuda, M., Murakami, Y. and Isida, M., 1985, "Stress Field by Interaction Effect of 2 Elliptical Inclusions," *Trans. J.S.M.E.*, Vol. 51, No. 464, pp. 1057~1065.